Nano Res. 2011, 4(6): 523–530
DOI 10.1007/s12274-011-0108-y
Research Article

ISSN 1998-0124
CN 11-5974/O4

Direct Imaging of Molecular Orbitals of Metal Phthalocyanines on Metal Surfaces with an O_2-Functionalized Tip of a Scanning Tunneling Microscope

Zhihai Cheng[1], Shixuan Du[1], Wei Guo[1], Li Gao[1], Zhitao Deng[1], Nan Jiang[1], Haiming Guo[1], Hao Tang[2], and H. -J. Gao[1] (✉)

[1] Institute of Physics, Chinese Academy of Sciences, P.O. Box 603, Beijing 100190, China
[2] Center for Material Elaboration and Structural Studies, B.P. 94347, 31055 Toulouse Cedex, France

Received: 10 July 2010 / Revised:12 January 2011 / Accepted: 12 January 2011

ABSTRACT

High-resolution scanning tunneling microscope images of iron phthalocyanine and zinc phthalocyanine molecules on Au(111) have been obtained using a functionalized tip of a scanning tunneling microscope (STM), and show rich intramolecular features that are not observed using clean tips. *Ab initio* density functional theory calculations and extended Hückel theory calculations revealed that the imaging of detailed electronic states is due specifically to the decoration of the STM tip with O_2. The detailed structures are differentiated only when interacting with the highly directional orbitals of the oxygen molecules adsorbed on a truncated, [111]-oriented tungsten tip. Our results indicate a method for increasing the resolution in generic scans and thus, have potential applications in fundamental research based on high-resolution electronic states of molecules on metals, concerning, for example, chemical reactions, and catalysis mechanisms.

KEYWORDS

High-resolution scanning tunneling microscope (STM) imaging, functionalized STM tip, metal phthalocyanines, molecular orbital, density functional theory calculation

1. Introduction

Organic functional molecules on solid surfaces have been extensively investigated with regard to both the fundamental aspects of the organic–inorganic interface at a single-molecule level and potential applications in molecular electronics [1–9]. A scanning tunneling microscope has proven to be an exceptional tool for the imaging, manipulation, modification, and spectroscopy of adsorbed molecules on solid surfaces [10, 11]. In this respect, researchers seek to image molecular structures with higher resolution, allowing direct observation of detailed molecular orbitals, thus, providing a deeper understanding of the molecule–substrate interaction and reactions at a sub-molecular or even atomic scale. This could be accomplished by decoupling molecules from the substrate, for example, using an ultrathin insulating film [12, 13], a molecular layer between molecules and a metal substrate [14, 15], physisorbed molecules [16], or a semiconductor substrate [17]. An alternative way to get high-resolution images of molecules is to functionalize the scanning

Address correspondence to hjgao@iphy.ac.cn

tunneling microscope (STM) tip by attaching a molecule at its apex [18–22]. It has been proven that adsorbates at the tip apex can change the chemical contrast of the molecular layer on metal surfaces [19, 22]. Also, a tip functionalized with CO or C_2H_4 has been found to increase the resolution of STM imaging of small molecules [20, 21]. The chemical structure can also be resolved by atomic force microscopy [23]. Reciprocally, the unexpected resolution and symmetry of experimental images could help to extract the realistic chemical composition and orientation of the tip from STM image simulations [24]. However, for large molecules less work has been done on directly imaging the molecular electronic structures in detail.

In this paper, we report our recent investigation of the electronic states of iron phthalocyanine (FePc) and zinc phthalocyanine (ZnPc) molecules on Au(111) by low-temperature STM combined with density functional theory (DFT) calculations and STM image simulations. With a special tip, STM images of FePc and ZnPc molecules on Au(111) reveal features not observed with a normal metallic tip. Theoretical simulations using a large number of possible STM tips with different geometries, compositions and contaminants identified only one realistic O_2 functionalized [111]-oriented tungsten tip. This identification was initially based on a systematic comparison between simulated and experimental STM images of FePc, and confirmed afterwards by simulating ZnPc images. The fact that this specific tip geometry and composition determined with one molecule and could be applied directly to another molecule strongly support the suggestion that the O_2 functionalization of a W(111) tip could be a method for increasing the resolution for molecules directly adsorbed on metal surfaces.

2. Experimental and calculation details

The experiments were performed with a low-temperature STM system (LT-STM, Omicron GmbH) in an ultrahigh vacuum (UHV) chamber with a base pressure of 1×10^{-10} mbar. The bare Au(111) surface was prepared by several cycles of Ar^+ ion sputtering and annealing to 700 K, until a clean surface was confirmed by STM imaging. FePc and ZnPc (Aldrich, 98+%) were thermally evaporated at 540 K with a molecular beam deposition–low energy electron diffraction (MBD–LEED) technique onto an Au(111) surface held at 370 K. Subsequently, the sample was cooled down to 5 K directly in the STM chamber [9]. The normal STM tips were electrochemically-etched polycrystalline tungsten tips. All STM images were recorded in a constant current mode at 5 K.

In order to gain a detailed understanding of observed high-resolution STM images, the experimental STM results were compared with simulations based on DFT calculations both for free molecules and molecules on the substrate. For free molecule calculations we used Gaussian 98 at B3LYP/6-31G* level. For molecules on Au(111), theoretical calculations were based on density functional theory, the Perdew–Wang exchange-correlation functional with generalized-gradient corrections [25], projector augmented waves (PAW) [26], and plane waves, as implemented in the Vienna *Ab-initio* Simulation Package (VASP) code [27, 28]. Due to the huge size of the unit cells we limited the calculations to only one k-point. The energy cutoff in the simulation was 400 eV, and the structures were relaxed until the net force on every atom was smaller than 0.02 eV/Å. STM images were calculated with the GREEN code [29, 30], a program based on the extended Hückel theory (EHT) [31, 32]. In this program, the tunneling current is calculated explicitly by applying the Landauer formula in which the transmission coefficient is evaluated through a Green's function approach. This allows the precise tip apex geometry and composition to be taken into account, which is essential in the present context.

3. Results and discussion

Both FePc and ZnPc are typical planar D_{4h} symmetric metal phthalocyanines (MPc) molecules, composed of a flat Pc skeleton with an iron or zinc ion in the central cavity (see the insets of Figs. 1(d) and 2(d)). Highly ordered FePc and ZnPc monolayers were fabricated on Au(111) [33]. Figure 1(a) shows a typical STM image of the highly ordered FePc monolayer on Au(111) obtained using a normal STM tip. The molecules prefer a commensurate superstructure with a quadratic unit cell. Each FePc molecule is recognized as a four-lobed "cross" structure with a central round protrusion as shown in Fig. 1(c). This

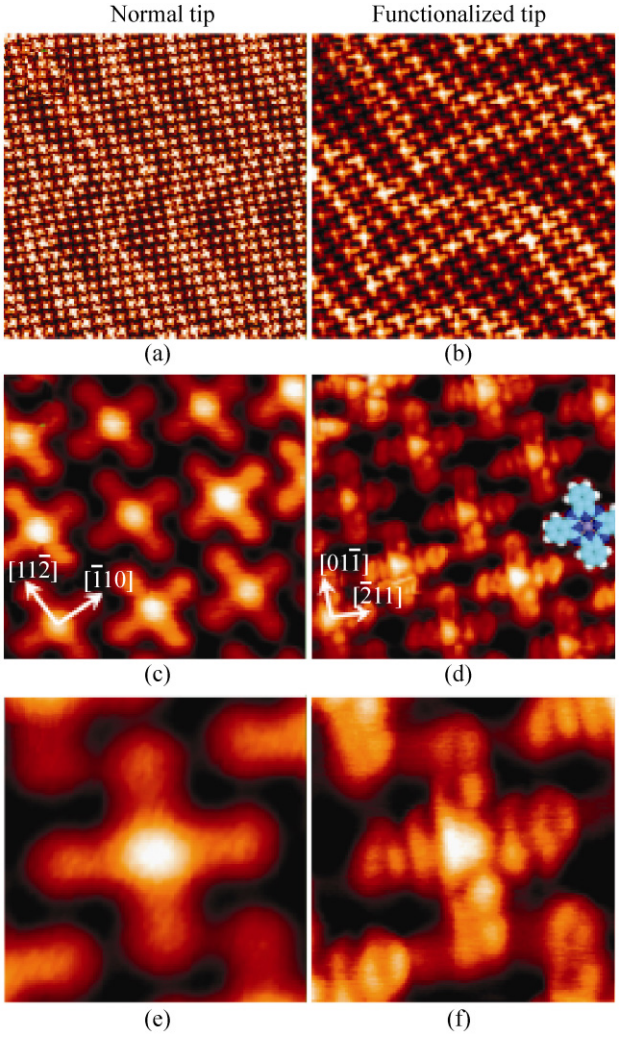

Figure 1 STM topographic images of an FePc monolayer on an Au(111) surface: (a) 40 nm × 40 nm; (b) 20 nm × 20 nm; (c) 5 nm × 5 nm; (d) 5 nm × 5 nm, structure of FePc as inset; (e) 2 nm × 2 nm; and (f) 2 nm × 2 nm. (a), (c), and (e) were obtained with a bare metallic STM tip. (b), (d), and (f) were obtained with a functionalized STM tip. All images were obtained with $V = -0.4$ V, $I = 0.05$ nA

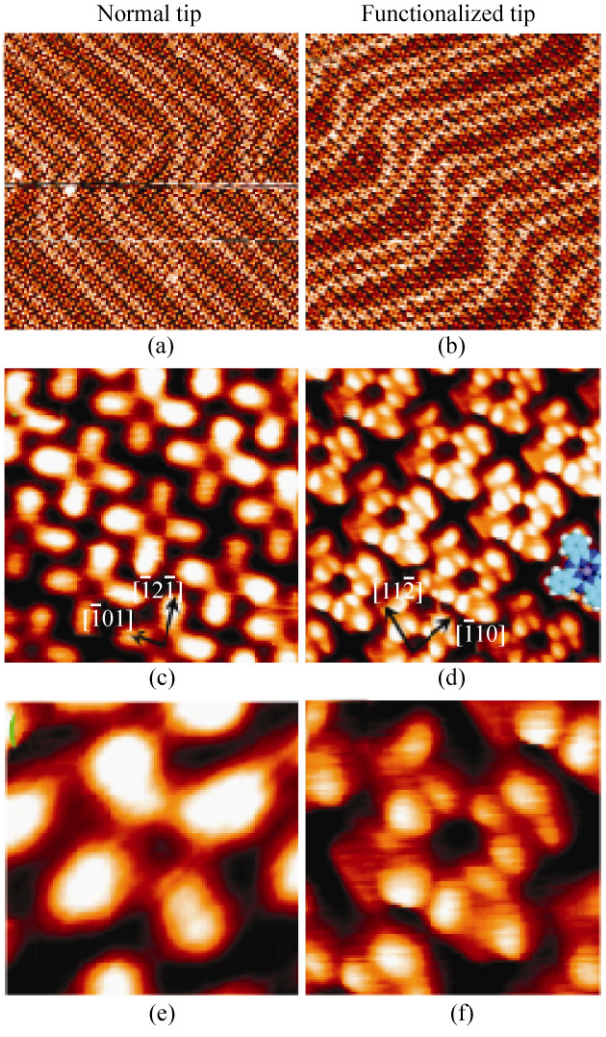

Figure 2 STM topographic images of a ZnPc monolayer on an Au(111) surface: (a) 40 nm × 40 nm; (b) 40 nm × 40 nm; (c) 5 nm × 5 nm; (d) 5 nm × 5 nm, structure of ZnPc as inset; (e) 2 nm × 2 nm; and (f) 2 nm × 2 nm. (a), (c), and (e) were obtained with a bare metallic STM tip. (b), (d), and (f) were obtained with a functionalized STM tip. All images were obtained with $V = -1.6$ V, $I = 0.05$ nA

indicates that the FePc molecules are in a flat-lying geometry on the terraces. The STM image of a highly ordered ZnPc monolayer is shown in Fig. 2(a), which shows a superstructure commensurate with the FePc monolayer. The ZnPc molecules also have a flat-lying adsorption configuration, and they are equally imaged as a four-lobed "cross" pattern with a normal STM tip, but the central zinc atom appears as a round hole as shown in Fig. 2(c), unlike FePc, whose central iron atom appears as a protrusion. Both FePc and ZnPc show identical orientations on Au(111), with the "cross" directed in the [1$\bar{1}$0] and [11$\bar{2}$] directions of the Au(111) surface.

The enhanced brightness at the center of FePc is ascribed to a large tunneling current that results from orbital-mediated tunneling through the half-filled d_{z^2} orbital of the Fe ion. In the case of ZnPc, the d orbitals of Zn are fully filled and there is no electronic state contributing to tunneling near the Fermi level [34–36]. Therefore the zinc ion of the ZnPc molecule appears as a hole in the STM images. Due to the three-fold symmetry of the Au(111) surface, the symmetry of the adsorbed planar MPc molecules is reduced from D_{4h} to C_{2v}.

Due to oxygen reduction by MPc species, some oxygen molecules will adsorb within the MPc powder

by virtue of the strong oxygen–MPc interactions [37–40]. So, a few oxygen molecules co-adsorb with the MPc molecules on the Au(111) surface during the deposition process. In the STM measurements, we purposely approach the MPc monolayer with the STM tip by either increasing the current or decreasing the bias so that the tip has a higher probability (compared with the normal scanning condition) of picking up an oxygen molecule. Then we have a small but non-zero chance of getting an O_2-functionalized STM tip. When introducing a few extra oxygen molecules to the chamber, we have a higher chance of getting an equivalent functionalized tip, directly confirming the O_2-functionalized STM tip from the experimental viewpoint.

Figures 1(b) and 2(b) present large scale STM images for FePc and ZnPc, respectively, on Au(111), with high resolution using the functionalized tip. Both FePc and ZnPc molecules can be resolved with many intramolecular features (see Figs. 1(d) and 2(d)) if this functionalized tip is used. Intramolecular features are revealed in the close-up STM images of FePc and ZnPc molecules, as presented in Figs. 1(f) and 2(f), respectively. The images obtained with the normal tip (Figs. 1(e) and 2(e)) are shown for comparison. The difference in the images of the FePc molecule is most pronounced for the central protrusion. This protrusion appears as a featureless round bump in images with the normal tip, while it appears as a nearly equilateral triangle with the functionalized tip. The specific features are also observed within the molecular lobes. Without considering the intensity asymmetry of different lobes, the features within the two lobes of FePc along the $[01\bar{1}]$ direction are mirrored in the $[\bar{2}11]$ direction, while those within the two lobes along the $[\bar{2}11]$ direction are also mirrored in the $[01\bar{1}]$ direction. But the features of lobes in different directions are different, similar to the highest occupied molecular orbital (HOMO) of a free FePc molecule, as shown in Fig. 3(a). It is apparent that the triangular protrusion at the iron position is different from the HOMO of a free FePc molecule, demonstrating the strong effect of the substrate on the central iron atom. So we can conclude that the interaction between the central iron atom and the substrate is the main contributor to the whole FePc molecule–substrate interaction. Furthermore, this triangular protrusion must be induced by the mismatch of symmetry of the FePc molecule and the Au(111) substrate.

As for the ZnPc molecule, the corresponding image retains the round central depression with the functionalized tip, even though the rest of the molecule is substantially better resolved than it would be with a normal tip. Each of its four lobes shows similar intramolecular features, in which each lobe is divided into four small protrusions with different intensity. This is also similar to the HOMO of an isolated ZnPc molecule (Fig. 3(b)). Unlike the FePc/Au(111) system, in which the adsorption changes the central protrusion from round to triangular, the center of ZnPc is still a round hole after adsorption. As the chemical structures of FePc and ZnPc are so similar, this difference must be attributed to their different molecule–substrate interactions resulting from their different central metal ions. That is to say, the interaction between Fe^{2+} and the substrate is stronger than that between Zn^{2+} and the substrate.

In order to fully understand the physical information behind these high-resolution STM images, we performed *ab initio* calculations for the adsorption of FePc (and ZnPc) on Au(111). STM images were simulated with the GREEN code using previously DFT-optimized FePc (ZnPc) monolayers on Au(111) with a realistic W(111) tip [41] (single atom terminated pyramid, Fig. 3(c), top view and side view) and a blunt tip (obtained by removing the end atom) with one O_2 molecule attached to it (Fig. 3(d), top view and side view). It is commonly assumed that no sub-molecular resolution is achievable with standard STM tips concerning a single molecule or a monolayer of adsorbed molecules on a metallic substrate. This is only possible if the molecules are positioned on a second layer or on an insulating "buffer" layer. The difference can be ascribed to the well-known alignment of molecular orbitals with the substrate Fermi level upon adsorption, or the fact that the molecular states are merged with the surface electrons to produce a convoluted STM image [14]. The alignment corresponds to a shift of molecular orbitals like the HOMOs and lowest unoccupied molecular orbitals (LUMOs) (see Scanning Tunneling Spectroscopy (STS) and VASP-calculated projected densities of states (PDOS), e.g., SnPc on Ag

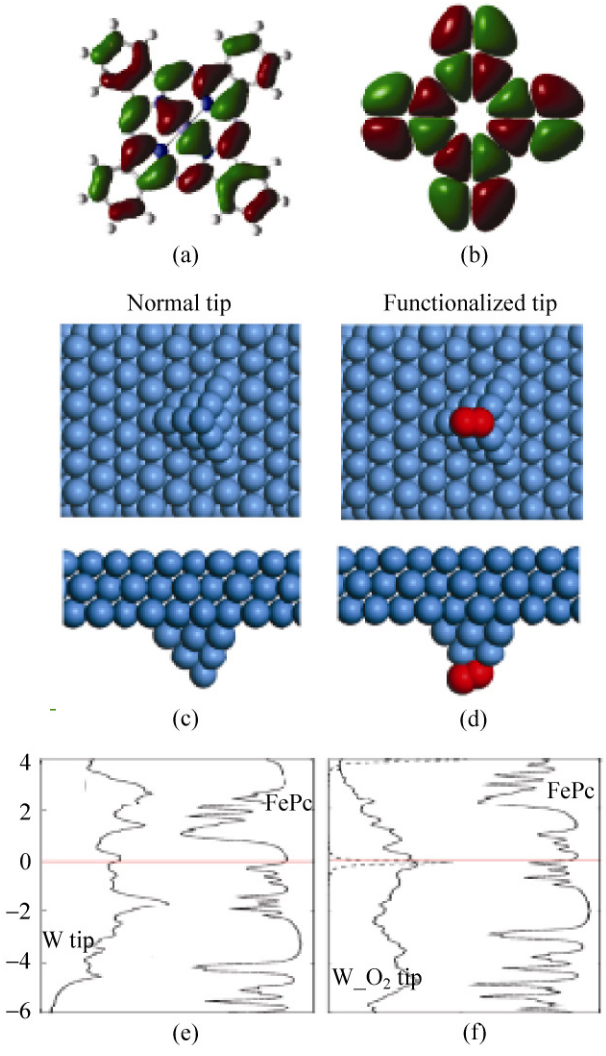

Figure 3 HOMOs of *M*Pc (*M* = Fe or Zn) and STM tips used in the simulations. (a) HOMO of FePc; (b) HOMO of ZnPc; (c) a sharp W(111) tip apex supported by a W slab: top view and side view; (d) O_2-functionalized blunt W(111) tip apex supported by a W slab: top view and side view (red balls are oxygen atoms); (e) PDOS for FePc on Au(111) and the pure W(111) tip; and (f) PDOS for FePc on Au(111) and the O_2-functionalized W(111) tip. The dashed lines are the DOS projected on O_2 molecule. The horizontal lines indicate the Fermi level

reported in Ref. [14]). The consequence is that these levels are out of range under standard bias (for example, 0.4 V and 1.6 V for imaging FePc and ZnPc, respectively) with the pure metallic STM tip. With the functionalized tip, however, the adsorption of molecules or impurities creates new localized electronic states that restore the bias range for a sub-molecular resolution. Here we take FePc/Au(111) as an example to illustrate this effect. The calculated PDOS of the FePc molecule on the Au(111) substrate (right hand panels of Figs. 3(e) and 3(f)) is presented with the PDOS of the clean tungsten tip (left hand panel of Fig. 3(e)) and with the PDOS of the O_2-functionalized tungsten tip (left hand panel of Fig. 3(f)), with respect to the bias used in simulation. It is clear that the oxygen atoms create a new localized electronic state near the Fermi level, which should make the intramolecular features of HOMO of FePc molecule visible.

Our simulation using a pyramidal W-fcc(111) oriented tip (a normal STM tip shown in Fig. 3(c)) shows a four-lobed "cross" structure with a round protrusion in the center for FePc/Au(111) (Fig. 4(a)). The simulation with the same tip also shows a "cross" structure with a round "hole" in the center for ZnPc/Au(111) (Fig. 4(c)). Both simulations are in good agreement with the experimental results (Figs. 1(e) and 2(e)). The simulations using a blunt tip with one O_2 molecule (the O_2-functionalized tip shown in Fig. 3(d)) show the intramolecular features within the FePc and ZnPc molecules (Figs. 4(b) and 4(d), respectively), which are in good agreement with the experimental

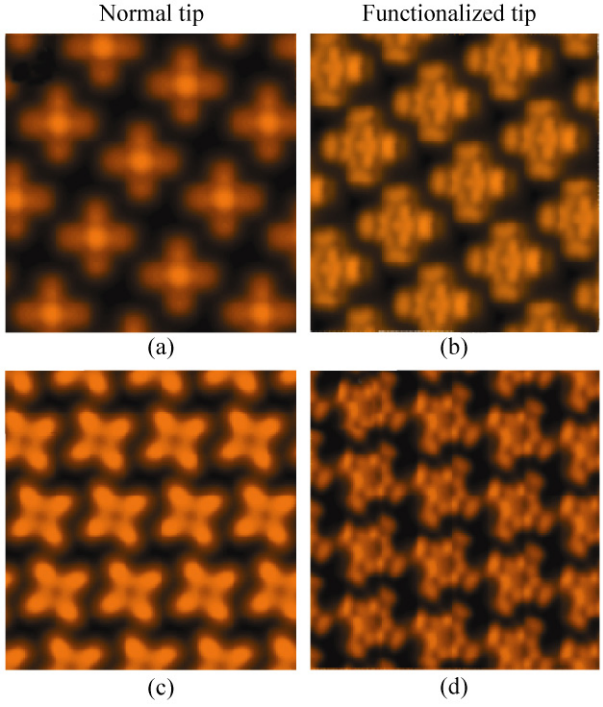

Figure 4 Simulated STM images using different tips. STM images of (a) FePc and (c) ZnPc on Au(111) simulated with a bare metallic STM tip; STM images of (b) FePc and (d) ZnPc on Au(111) simulated with an O_2-functionalized STM tip

results presented in Figs. 1(f) and 2(f), especially the asymmetry inside each lobe of the molecular orbital resolved images.

Finally, we want to stress that during our experiments, after we reduced the tip–surface distance to pick up a molecule in order to functionalize the tip, we did not find any MPc molecules missing from the MPc monolayer. Based on this direct experimental evidence, we can exclude the possibility of an MPc-functionalized STM tip. Although the possibility of contaminants (of compositions Au, W, O, N, C, NO, CO, N_2, or O_2) is negligible, we have systematically compared STM images simulated with these contaminants on different tips such as W-fcc(111), W-bcc(110), and Au-fcc(111). Two examples of STM tips, a W(110) tip (Fig. 5(a)) and an N_2-functionalized W(111) tip (Fig. 5(b)), and the corresponding simulated STM images for the FePc/Au(111) system obtained with these tips are shown in Figs. 5(c) and 5(d), respectively. Of all the calculated images, only the one calculated with an O_2-functionalized W(111) tip was in close agreement with the experimental observations. Once this unique geometry and composition has been determined, we have verified by calculation that a rotation of 120° of the O_2 at the extremity of the apex does not introduce any significant modification in the simulated image. As this same functionalized tip was used directly to simulate STM images for ZnPc/Au(111) with excellent agreement with experiment, we may conclude that the special functionalized tip in the experiments was indeed modified by oxygen molecules at the tip apex.

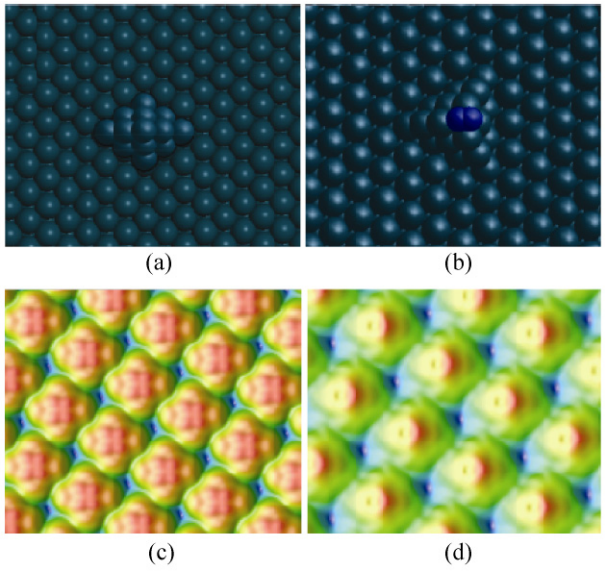

Figure 5 Different STM tips and the corresponding simulated STM images. (a) W(110) tip; (b) N_2-functionalized W(111) tip (blue balls are nitrogen atoms); (c) simulated STM image for FePc/Au(111) using the W(110) tip; (d) simulated STM image for FePc/Au(111) using the N_2-functionalized W(111) tip

4. Conclusions

We have investigated the electronic states of FePc and ZnPc molecules on an Au(111) surface by a combination of low-temperature STM analysis and DFT and ETH calculations. High-resolution STM images of FePc and ZnPc molecules on Au(111) are obtained using functionalized tips, by means of which intramolecular features are observable within the molecules. The key difference between a clean tip and a molecule-covered tip was found to be the energetic registry between tip orbitals and orbitals of the molecules at the surface. The experimental results and their interpretation are in excellent agreement with simulated STM images based on the DFT and ETH calculations. Our results indicate that when well controlled, the technique of functionalizing a tungsten tip by O_2 molecules could be a simple solution to improve the resolution of STM images of large molecules on metal surfaces.

Acknowledgements

This project is supported by the Natural Science Foundation of China (NSFC), the Chinese National "973" project of the Ministry of Science and Technology (MOST), the Chinese Academy of Sciences and the Shanghai Supercomputer Center. H. T. acknowledges the "Centre de Calcul en Midi-Pyrenees" (CALMIP) for computational resources. H. T. also thanks Sébastien Gauthier for useful discussions.

References

[1] Gimzewski, J. K; Joachim, C. Nanoscale science of single molecules using local probes. *Science* **1999**, *283*, 1683–1688.

[2] Crone, B.; Dodabalapur, A.; Lin, Y. Y.; Filas, R. W.; Bao, Z.; LaDuca, A.; Sarpeshkar, R.; Katz, H. E.; Li, W. Large-scale complementary integrated circuits based on organic transistors.

Nature **2000**, *403*, 521–523.

[3] Joachim, C.; Gimzewski, J. K.; Aviram, A. Electronics using hybrid-molecular and mono-molecular devices. *Nature* **2000**, *408*, 541–548.

[4] Barth, J. V.; Weckesser, J.; Cai, C.; Günter, P.; Bürgi, L.; Jeandupeux, O.; Kern, K. Building supramolecular nanostructures at surfaces by hydrogen bonding. *Angew. Chem. Int.* Ed. **2000**, *39*, 1230–1234.

[5] Gao, H. J.; Sohlberg, K.; Xue Z. Q.; Chen, H. Y.; Hou, S. M.; Ma, L. P.; Fang, X. W.; Pang, S. J.; Pennycook, S. J. Reversible, nanometer-scale conductance transitions in an organic complex. *Phys. Rev. Lett.* **2000**, *84,* 1780–1783.

[6] Rosei, F.; Schunack, M.; Naitoh, Y.; Jiang, P.; Gourdon, A.; Laegsgaard, E.; Stensgaard, I.; Joachim, C.; Besenbacher, F. Properties of large organic molecules on metal surfaces. *Prog. Surf. Sci.* **2003**, *71*, 95–146.

[7] Feng, M.; Guo, X. F.; Xin, L.; He, X. B.; Ji, W.; Du, S. X.; Zhang, D. Q.; Zhu, D. B.; Gao, H. J. Stable, reproducible nanorecording on rotaxane thin films. *J. Am. Chem. Soc.* **2005**, *127*, 15338–15339.

[8] Du, S. X.; Gao, H. J.; Seidel, C.; Tsetseris, L.; Ji, W.; Kopf, H.; Chi, L. F.; Fuchs, H.; Pennycook, S. J.; Pantelides, S. T. Selective nontemplated adsorption of organic molecules on nanofacets and the role of bonding patterns. *Phys. Rev. Lett.* **2006**, *97*, 156105.

[9] Gao, H. J.; Gao, L. Scanning tunneling microscopy of functional nanostructures on solid surfaces: Manipulation, self-assembly, and applications. *Prog. Surf. Sci.* **2009**, *85*, 28–91.

[10] Kaiser, W. J.; Stroscio, J. A. *Scanning Tunneling Microscopy*, in *Methods of Experimental Physics*. Celotta, R.; Lucatorto, T., Eds.; Academic Press: San Diego, 1993; Vol. 27.

[11] Foster, A. S.; Hofer, W. A. *Scanning Probe Microscopy: Atomic Scale Engineering by Forces and Currents*; Springer: New York, 2006.

[12] Repp, J.; Meyer, G.; Stojković, S. M.; Gourdon, A.; Joachim, C. Molecules on insulating films: Scanning-tunneling microscopy imaging of individual molecular orbitals. *Phys. Rev. Lett.* **2005**, *94*, 026803.

[13] Scarfato, A.; Chang, S. H.; Kuck, S.; Brede, J.; Hoffmann, G.; Wiesendanger, R. Scanning tunneling microscope study of iron(II) phthalocyanine growth on metals and insulating surfaces. *Surf. Sci.* **2008**, *602*, 677–683.

[14] Wang, Y.; Krögeer, J.; Berndt, R.; Hofer, W. Structural and electronic properties of ultrathin tin phthalocyanine films on Ag(111) at the single-molecule level. *Angew. Chem. Int. Ed.* **2009**, *48*, 1261–1263.

[15] Ge, X.; Manzano, C.; Berndt, G.; Anger, L. T.; Köhler, F.; Herges, R. Controlled formation of an axially bonded Co-phthalocyanine dimer. *J. Am. Chem. Soc.* **2009**, *131*, 6096–6098.

[16] Soe, W. H.; Manzano, C.; De Sarkar, A.; Chandrasekhar, N.; Joachim, C. Direct observation of molecular orbitals of pentacene physisorbed on Au(111) by scanning tunneling microscope. *Phys. Rev. Lett.* **2009**, *102*, 176102.

[17] Bellec, A.; Ample, F.; Riedel, D.; Dujardin, G.; Joachim, C. Imaging molecular orbitals by scanning tunneling microscopy on a passivated semiconductor. *Nano Lett.* **2009**, *9*, 144–147.

[18] Eigler, D. M.; Lutz, C. P.; Rudge, W. E. An atomic switch realized with the scanning tunneling microscope. *Nature* **1991**, *352*, 600–603.

[19] Bartels, L.; Meyer, G.; Rieder, K. H. Controlled vertical manipulation of single CO molecules with the scanning tunneling microscope: A route to chemical contrast. *Appl. Phys. Lett.* **1997**, *71*, 213–215.

[20] Bartels, L.; Meyer, G.; Rieder, K. H. The evolution of CO adsorption on Cu(111) as studied with bare and CO-functionalized scanning tunneling tips. *Surf. Sci.* **1999**, *432*, L621–L626.

[21] Haln, J. R.; Ho, W. Single molecule imaging and vibrational spectroscopy with a chemically modified tip of a scanning tunneling microscope. *Phys. Rev. Lett.* **2001**, *87*, 196102.

[22] Deng, Z. T.; Lin, H.; Ji, W.; Gao, L.; Lin, X.; Cheng, Z. H.; He, X. B.; Lu, J. L.; Shi, D. X.; Hofer, W. A.; Gao, H. J. Selective analysis of molecular states by functionalized scanning tunneling microscopy tips. *Phys. Rev. Lett.* **2006**, *96*, 156102.

[23] Gross, L.; Mohn, F.; Moll, N.; Liljeroth, P.; Meyer, G. The chemical structure of a molecule resolved by atomic force microscopy. *Science* **2009**, *325*, 1110–1114.

[24] Hagelaar, J. H. A.; Flipse, C. F.; Cerda, J. L. Modeling realistic tip structures: Scanning tunneling microscopy of NO adsorption on Rh(111). *Phys. Rev. B* **2008**, *78*, 161405(R).

[25] Perdew, J. P.; Chevary, J. A.; Vosko, S. H.; Jackson, K. A.; Pederson, M. R.; Singh, D. J.; Jiolhais, C. Atoms, molecules, solids, and surfaces: Applications of the generalized gradient approximation for exchange and correlation. *Phys. Rev. B* **1992**, *46*, 6671–6687.

[26] Blöchl, E. Projector augmented-wave method. *Phys. Rev. B* **1994**, *50*, 17953–17979.

[27] Kresse, G.; Hafner, J. *Ab initio* molecular dynamics for liquid metals. *Phys. Rev. B* **1993**, *47*, 558–561.

[28] Kresse, G.; Furthmüller, J. Efficient iterative schemes for *ab initio* total-energy calculations using a plane-wave basis set. *Phys. Rev. B* **1996**, *54*, 11169–11186.

[29] Cerdá, J.; Van Hove, M. A.; Sautet, P.; Salmeron, M. Efficient method for the simulation of STM images. I. Generalized green-function formalism. *Phys. Rev. B* **1997**, *56*, 15885–15899.

[30] Cerdá, J.; Yoon, A.; Van Hove, M. A.; Sautet, P.; Salmeron, M.; Somorjai, G. A. Efficient method for the simulation of STM images. II. Application to clean Rh(111) and Rh(111)+ c(4×2)-2S. *Phys. Rev. B* **1997**, *56*, 15900–15918.

[31] Hoffmann, R. An extended Hückel theory. I. Hydrocarbons. *J. Chem. Phys*.**1963**, *39*, 1397–1412.

[32] Cerdá, J.; Soria, F. Accurate and transferable extended Hückel-type tight-binding parameters. *Phys. Rev. B* **2000**, *61*, 7965–7971.

[33] Cheng, Z. H.; Gao, L.; Deng, Z. T.; Liu, Q.; Jiang, N.; Lin, X.; He, X. B.; Du, S. X.; Gao, H. J. Epitaxial growth of iron phthalocyanine at the initial stage on Au(111) surface. *J. Phys. Chem. C* **2007**, *111*, 2656–2660.

[34] Lu, X.; Hipps, K. W. Scanning tunneling microscopy of metal phthalocyanines: d^6 and d^8 cases. *J. Phys. Chem. B* **1997**, *101*, 5391–5396.

[35] Yoshimoto, S.; Tsutsumi, E.; Suto, K.; Honda, Y.; Itaya, K. Molecular assemblies and redox reactions of zinc(II) tetraphenylporphyrin and zinc(II) phthalocyanine on Au(111) single crystal surface at electrochemical interface. *Chem. Phys.* **2005**, *319*, 147–158.

[36] Liao, M. S.; Scheiner, S. Electronic structure and bonding in metal phthalocyanines, metal = Fe, Co, Ni, Cu, Zn, Mg. *J. Chem. Phys.* **2001**, *114*, 9780–9791.

[37] Bohrer, F. I.; Sharoni, A.; Colesniuc, C.; Park, J.; Schuller, I. K.; Kummel, A. C.; Trogler, W. C. Gas sensing mechanism in chemiresistive cobalt and metal-free phthalocyanine thin films. *J. Am. Chem. Soc.* **2007**, *129*, 5640–5646.

[38] Sabelli, N. H.; Melendres, C. A. Comparative semiempirical study of oxygen binding to model iron complexes of phthalocyanine and porphyrin. *J. Phys. Chem.* **1982**, *86*, 4342–4346.

[39] Zhivkov, I. Oxygen induced charge carrier generation and trapping in vacuum deposited phthalocyanine thin films. *J. Optoelectr. and Adv. Mater.* **2009**, *11*, 1396–1399.

[40] Dahlberg, S. C.; Musser, M. E. Electron acceptor surface states due to oxygen adsorption on metal phthalocyanine films. *J. Chem. Phys.* **1980**, *72*, 6706–6711.

[41] Lucier, A. S.; Mortensen, H.; Grütter P. Determination of the atomic structure of scanning probe microscopy tungsten tips by field ion microscopy. *Phys. Rev. B* **2005**, *72*, 235420.